Journal of Sound and Vibration (2001) **244**(4), 569–581
doi:10.1006/jsvi.2000.3510, available online at http://www.idealibrary.com on IDEAL®

AN IMPROVED ROTOR MODEL WITH EQUIVALENT DYNAMIC EFFECTS OF THE SUPPORT STRUCTURE

B. L. Choi and J. M. Park

Department of Mechanical Engineering and Applied Mechanics, Korea University, 5-1 *Anam, Sungbuk-Gu, Seoul, Korea. E-mail: topmount@shinbiro.com*

(*Received* 29 *February* 2000, *and in final form* 30 *June* 2000)

Dynamic effects of the support structure are important in vibration analyses of a rotor. It may well happen in real machines such as centrifugal pumps or turbines operating on a flexible structure. This paper suggests an improved rotor model for including the support effects efficiently into the rotor-bearing system. The support FRFs are used to extract the spring–mass models which have the same dynamic characteristics of the support structure. These regenerated models are directly inserted into the rotor. On the other hand, the impedance coupling method, which is often used in structural vibration problems, is presented to verify the suggested modelling technique. It is based on the FRFs of each substructure and the constraint conditions of interface co-ordinates. To demonstrate the applicability and validity of the analytical procedures, they are applied to the rotor of a double suction centrifugal pump. As a result, they show a good agreement with each other.

1. INTRODUCTION

A structure of turbomachinery such as a pump and a turbine can be divided into the rotor and the stator. Many published works are interested in the critical speed, instability, and vibration behaviors of the rotor due to the mechanical unbalance or the self-excited sources. These dynamic characteristics of the rotor have been successfully analyzed using the finite element method or the transfer matrix method [1–6], and well established theoretically [7, 8].

But, most of the presented papers ignore the dynamic effects of the support structure or deal with a simple *shaft–impeller-bearing* system. These cannot represent the dynamic behaviors of the real system very well, because the rotor vibrations are strongly dependent upon the dynamic stiffness and the stiffness asymmetry of the support structure [9, 10].

In order to perform the dynamic analysis of the complex system efficiently, several methods have been widely used in structural vibration problems. One of the most common techniques is the dynamic stiffness matrix method [11, 12], which converts the compliance FRFs to the dynamic stiffness matrix at discrete frequencies. The transformed matrix is directly inserted into the global matrix at an appropriate degree of freedom. Yang [13] presented the characteristic equation of the system in terms of the transfer functions of the component systems and the transfer functions describing the combined gyroscopic system. Suarez *et al.* [14] used a modal synthesis method to calculate the lower eigenproperties of a general dynamic system divided into subsystems. Taiping [15] presented the transfer matrix impedance coupling method for calculating the eigensolutions of multi-spool rotor systems.

0022-460X/01/290569 + 13 $35.00/0

This paper presents the applications of the impedance coupling method and the improved rotor model. The former is well established and generalized mathematically, and it is applied to couple some co-ordinates in several substructures. So, its results can be used to verify the other analytical method. On the other hand, the latter is an efficient modelling technique for including the support effects into the rotor model. The FRFs of the support structure are calculated using MSC/NASTRAN by the finite element method. They are used to extract the spring–mass models, which have the same dynamic characteristics of the support structure. These regenerated models are directly inserted into the rotor. To demonstrate the validity of the analysis procedures provided, they are applied to the rotor of the double suction centrifugal pump.

2. FREQUENCY RESPONSE FUNCTION AND DESCRIPTION OF THE SYSTEM

2.1. FREQUENCY RESPONSE FUNCTION

Dynamic characteristics of a structural system may be described by several different models as follows. The spatial model is given by $[M]$, $[C]$, and $[K]$ which can be constructed through an analytical technique. It leads to an eigenproblem, which yields the modal model constituted by natural frequencies, damping values, and mode shapes. Furthermore, the modal model can be reconstructed to establish the response model.

Experimental modal analysis is also a very useful tool in a complex structure. It has been well known that the modal model can be extracted from the response model. Normally, test results are represented as transfer functions by means of artificial excitation. From the modal model, the equivalent properties such as mass, stiffness, and damping matrices can be estimated.

The equation of motion for a linear and damped structure can be generalized as

$$[M]\{\ddot{x}(t)\} + [C]\{\dot{x}(t)\} + [K]\{x(t)\} = \{f(t)\}, \tag{1}$$

where $[M]$, $[C]$, and $[K]$ are the mass, damping, and stiffness matrices of the structure respectively. $\{f(t)\}$ is the time-dependent force vector and $\{x(t)\}$ is the displacement vector. The steady state solutions are obtained by assuming that the excitation forces are $\{f(t)\} = \{F(\omega)\}\,e^{j\omega t}$ and the responses also have the same frequency as $\{x(t)\} = \{X(\omega)\}\,e^{j\omega t}$.

Thus, the dynamic responses are characterized by the following matrix equation:

$$\{X(\omega)\} = ([K] - \omega^2[M] + j\omega[C])^{-1}\{F(\omega)\} \tag{2}$$

or

$$\{X(\omega)\} = [H(\omega)]\{F(\omega)\}, \tag{3}$$

where

$$[H(\omega)]^{-1} = ([K] - \omega^2[M] + j\omega[C]). \tag{4}$$

In equation (4), premultiply both sides by $[\Phi]^T$ and postmultiply both sides by $[\Phi]$. Then, by taking the orthogonality properties of the eigenvectors and the inverse relationships, it may be concluded that

$$[H(\omega)] = [\Phi]\begin{pmatrix} \ddots & & \\ & \omega_r^2 - \omega^2 + j2\xi_r\omega_r\omega & \\ & & \ddots \end{pmatrix}^{-1}[\Phi]^T \tag{5}$$

or

$$H_{jk}(\omega) = \sum_{r=0}^{n} \frac{{}_r\phi_j \, {}_r\phi_k}{\omega_r^2 - \omega^2 + \mathrm{j}2\xi_r\omega_r\omega}, \tag{6}$$

where

$$[\Phi]^{\mathrm{T}}[M][\Phi] = [I],$$

$$[\Phi]^{\mathrm{T}}[K][\Phi] = \begin{bmatrix} \ddots & & \\ & \omega_r^2 & \\ & & \ddots \end{bmatrix},$$

$$[\Phi]^{\mathrm{T}}[C][\Phi] = \begin{bmatrix} \ddots & & \\ & 2\xi_r\omega_r & \\ & & \ddots \end{bmatrix}. \tag{7}$$

The matrix $[H(\omega)]$ is commonly denoted as a frequency response matrix relating the input excitations to the output responses. If we are interested in extracting a single element, i.e., the response at co-ordinate "j" due to a single harmonic force at co-ordinate "k", this means that the force vector will have just one non-zero element and therefore we can write as follows:

$$H_{jk}(\omega) = \frac{X_j(\omega)}{F_k(\omega)}, \qquad F_m = 0 \quad \text{and} \quad m \neq k. \tag{8}$$

In particular, damping terms can be neglected for undamped or lightly damped structures. So, the magnitude of typical individual FRF would be expected to have the form of a ratio of two polynomials as [16]

$$|H_{jk}(\omega)| = \left| \frac{b_0 + b_1\omega^2 + \cdots + b_{n-1}\omega^{2n-2}}{a_0 + a_1\omega^2 + \cdots + a_{n-1}\omega^{2n-2} + a_n\omega^{2n}} \right|. \tag{9}$$

It is clear that the roots in the denominator are natural frequencies of the structure determined by $|[K] - \omega^2[M]| = 0$, and the roots in the numerator represent frequencies at anti-resonances. Therefore, equation (9) can also be expressed as follows:

$$|H_{jk}(\omega)| = \left| B \frac{(\Omega_1^2 - \omega^2)\cdots(\Omega_{n-1}^2 - \omega^2)}{(\omega_1^2 - \omega^2)\cdots(\omega_{n-1}^2 - \omega^2)(\omega_n^2 - \omega^2)} \right|. \tag{10}$$

2.2. SUBSTRUCTURE MODELS OF THE PUMP SYSTEM

In order to support later developments, an explanation of each substructure is presented. Figure 1 shows a finite element model of the double suction centrifugal pump. A fixed co-ordinate reference system, with the X-axis coinciding with the undeformed centerline of the shaft, is used to describe the system configuration. The specification of the pump is listed in Table 1.

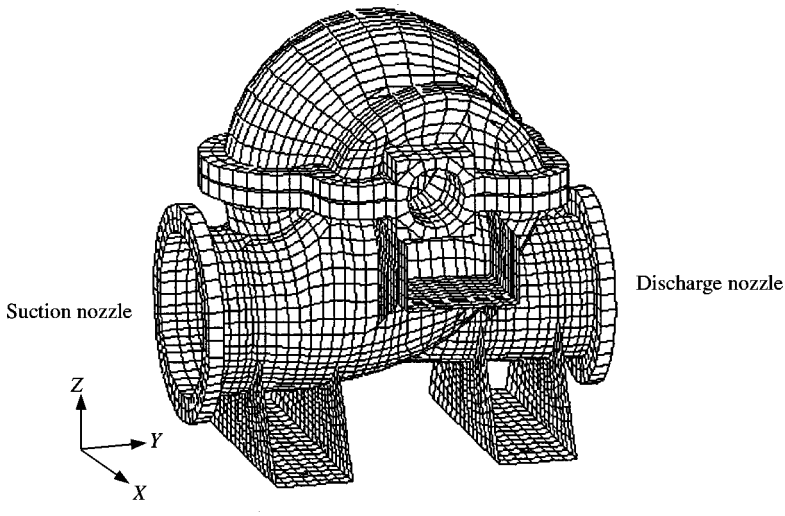

Figure 1. Finite element model of the double suction centrifugal pump.

TABLE 1

Specification of the double suction centrifugal pump

Specification	Double suction, single stage, radially splitted type centrifugal pump	
Pump size (in)	$16 \times 14 - 16$	
Design condition (at BEP)	Flow	2500 m^3/h
	Head	50 m
	Power	520 kW
	r.p.m.	1800 r.p.m.

2.2.1. *Rotor*

The mathematical rotor model consists of beams, lumped mass, and bearings. It includes the effects of translational and rotatory inertia, gyroscopic moment, bending and shear deformations. The governing equations of the rotor system are well established by many authors [17–20]. The responses of a rotor are influenced strongly by bearing effects, and, especially, instability may also occur by self-excited vibrations arising from the fluid film of journal bearings [21]. But, in rolling element bearings, forces are purely elastic, i.e., produced by elastic contact deformation of the balls, of the races, and of the bearing housing structure. An appropriate model for this type of bearing is a linear or non-linear spring with no damping and no cross-coupling [22].

In this example, the ball bearings are used to support the rotor and their isotropic properties are listed in Table 2. These bearing properties can, therefore, be directly included into the rotor.

2.2.2. *Dynamic properties of the support structure*

The support structure consists of a pump casing, a pedestal, and a foundation. Its dynamic properties are important in rotor vibrational analyses. In order to obtain the

TABLE 2

Rotor configuration data

Material properties	
Young's modulus	$E = 19{,}200$ MPa
Density	$\rho = 7860$ kg/m^3
Rigid disk	
Mass	$M_D = 53{\cdot}90$ kg
Polar mass moment of inertia	$I_P = 0{\cdot}968$ kg m^2
Diametral mass moment of inertia	$I_D = 0{\cdot}750$ kg m^2
Bearing stiffness	
Radial bearing	$k_{yy}(= k_{zz}) = 2{\cdot}76 \times 10^8$ N/m
Thrust bearing	$k_{yy}(= k_{zz}) = 5{\cdot}03 \times 10^8$ N/m

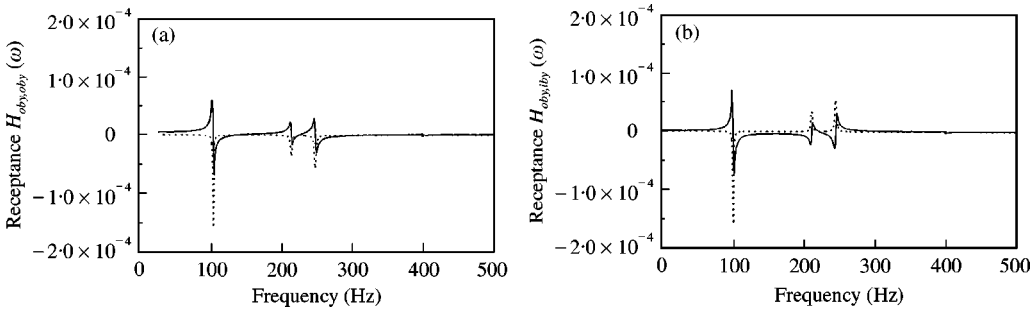

Figure 2. FRFs at the outboard bearing position (a) the driving FRF, (b) the transfer FRF: ——, real; ·····, imaginary.

support dynamics analytically, it is necessary to perform the frequency response analysis. Figure 2 shows the receptances of the support model. Where, the driving point FRF means the co-ordinates of the response and the force are the same, whereas, the transfer FRF means the response at the out-board bearing due to a harmonic force at the in-board bearing. The matrix equation is as follows:

$$\{X(\omega)\}^{(s)} = [H(\omega)]^{(s)}\{F(\omega)\}^{(s)}, \tag{11}$$

where

$$\{X(\omega)\}^{(s)} = \begin{pmatrix} X_{oby} \\ X_{iby} \\ X_{obz} \\ X_{ibz} \end{pmatrix}, \quad [H(\omega)]^{(s)} = \begin{bmatrix} H_{oby,oby} & H_{oby,iby} & H_{oby,obz} & H_{oby,ibz} \\ H_{iby,oby} & H_{iby,iby} & H_{iby,obz} & H_{iby,ibz} \\ H_{obz,oby} & H_{obz,iby} & H_{obz,obz} & H_{obz,ibz} \\ H_{ibz,oby} & H_{ibz,iby} & H_{ibz,obz} & H_{ibz,ibz} \end{bmatrix}, \quad \{F(\omega)\}^{(s)} = \begin{pmatrix} F_{oby} \\ F_{iby} \\ F_{obz} \\ F_{ibz} \end{pmatrix}.$$

The supscript (s) indicates the support structure, and the subscripts *ib* and *ob* represent the in-board and out-board bearing positions respectively. In this model, the effects of forces perpendicular to each response are small, so the complex displacements can be approximated as

$$\begin{aligned} X_{oby} = X_{iby} &\doteqdot F_{ey}\{Re[H_{oby,oby} + mH_{oby,iby}] + Im[H_{oby,oby} + mH_{oby,iby}]\}, \\ X_{obz} = X_{ibz} &\doteqdot F_{ez}\{Re[H_{obz,obz} + mH_{obz,ibz}] + Im[H_{obz,obz} + mH_{obz,ibz}]\}, \end{aligned} \tag{12}$$

where X_{oby} and X_{obz} are the displacements neglecting the orthogonal effects in a symmetric model, and "m" indicates whether we consider the transfer FRF or not. These FRFs will be used to extract the spring–mass models, which have the same dynamic characteristics of the support structure.

3. FORMULATION OF SYNTHESIS MODEL

3.1. IMPEDANCE COUPLING METHOD

At first, impedance coupling method is presented to verify later suggested methodology. It makes use of the FRFs of each substructure, and they can be assembled into a matrix form to generate the full system [23–25]. The basic conditions in this coupling process are compatibility and equilibrium. So, the co-ordinates involved in the connection areas should be identified.

Let us consider the double suction centrifugal pump shown in Figure 1, where separate models can be assumed as rotor and support with orders n_1 and n_2 respectively. The rotor is a free condition and the support structure is constrained in a way depending upon the pump installation. The bearing positions connecting the two bodies are denoted by "c", and the remaining ones of each substructure are denoted by "r". Then, the equation of the rotor becomes

$$\begin{pmatrix} \{X_r^{(1)}\} \\ \{X_c^{(1)}\} \end{pmatrix} = \begin{bmatrix} [H_{(rr)}^{(1)}] & [H_{(rc)}^{(1)}] \\ [H_{(cr)}^{(1)}] & [H_{(cc)}^{(1)}] \end{bmatrix} \begin{pmatrix} \{F_r^{(1)}\} \\ \{F_c^{(1)}\} \end{pmatrix} \tag{13}$$

and that of the support structure is

$$\begin{pmatrix} \{X_c^{(2)}\} \\ \{X_r^{(2)}\} \end{pmatrix} = \begin{bmatrix} [H_{(cc)}^{(2)}] & [H_{(cr)}^{(2)}] \\ [H_{(rc)}^{(2)}] & [H_{(rr)}^{(2)}] \end{bmatrix} \begin{pmatrix} \{F_c^{(2)}\} \\ \{F_r^{(2)}\} \end{pmatrix}. \tag{14}$$

From equations (13) and (14), the equation of the assembled structure is formulated as

$$\{X^{(A)}\} = [H^{(A)}(\omega)]\,\{F^{(A)}\}, \tag{15}$$

where

$$[H^{(A)}(\omega)] = \begin{bmatrix} [H_{\alpha\alpha}] & [H_{\alpha\beta}] & [H_{\alpha\gamma}] \\ [H_{\beta\alpha}] & [H_{\beta\beta}] & [H_{\beta\gamma}] \\ [H_{\gamma\alpha}] & [H_{\gamma\beta}] & [H_{\gamma\gamma}] \end{bmatrix}.$$

The derivation of equation (15), which is the relation between displacement $\{X^{(A)}\}$ and force $\{F^{(A)}\}$ of the total structure, is the purpose of the impedance coupling process.

The conditions of displacement compatibility and equilibrium forces are as follows:

$$\{X_c^{(1)}\} = \{X_c^{(2)}\} = \{X_\beta^{(A)}\}, \qquad \{F_c^{(1)}\} + \{F_c^{(2)}\} = \{F_\beta^{(A)}\}. \tag{16}$$

In addition to equation (16), the forces and displacements at non-coupled co-ordinates on the assembled structure and substructures must be the same as the following forms:

$$\begin{aligned} \{F_\alpha^{(A)}\} &= \{F_r^{(1)}\}, \qquad \{F_\gamma^{(A)}\} = \{F_r^{(2)}\}, \\ \{X_\alpha^{(A)}\} &= \{X_r^{(1)}\}, \qquad \{X_\gamma^{(A)}\} = \{X_r^{(2)}\}. \end{aligned} \tag{17}$$

So, the connection coordinates of the assembled structure are

$$\begin{aligned}\{X_\beta^{(A)}\} &= [H_{\beta\alpha}]\{F_\alpha^{(A)}\} + [H_{\beta\beta}]\{F_\beta^{(A)}\} + [H_{\beta\gamma}]\{F_\gamma^{(A)}\} \\ &= [H_{cr}^{(1)}]\{F_r^{(1)}\} + [H_{cc}^{(1)}]\{F_c^{(1)}\} \\ &= [H_{cc}^{(2)}]\{F_c^{(2)}\} + [H_{cr}^{(2)}]\{F_r^{(2)}\}.\end{aligned} \tag{18}$$

From equations (16)–(18), $\{F_c^{(2)}\}$ can be expressed as

$$\{F_c^{(2)} = [[H_{cc}^{(1)}] + [H_{cc}^{(2)}]]^{-1}\{[H_{cr}^{(1)}]\{F_\alpha^{(A)}\} + [H_{cc}^{(1)}]\{F_\beta^{(A)}\} - [H_{cr}^{(2)}]\{F_\gamma^{(A)}\}\}. \tag{19}$$

Substituting equation (19) into the second row of equation (18), the following equation will be obtained

$$\begin{aligned}\{X_\beta^{(A)}\} &= [H_{cr}^{(1)}]\{F_\alpha^{(A)}\} + [H_{cc}^{(1)}]\{F_\beta^{(A)}\} \\ &\quad - [H_{cc}^{(1)}][[H_{cc}^{(1)}] + [H_{cc}^{(2)}]]^{-1}\{[H_{cr}^{(1)}]\{F_\alpha^{(A)}\} + [H_{cc}^{(1)}]\{F_\beta^{A}\} - [H_{cr}^{(2)}]\{F_\gamma^{(A)}\}\}\end{aligned} \tag{20}$$

or

$$\begin{aligned}\{X_\beta^{(A)}\} &= \{[H_{cr}^{(1)}] - [H_{cc}^{(1)}][[H_{cc}^{(1)}] + [H_{cc}^{(2)}]]^{-1}[H_{cr}^{(1)}]\}\{F_\alpha^{(A)}\} \\ &\quad + \{[H_{cc}^{(1)}] - [H_{cc}^{(1)}][[H_{cc}^{(1)}] + [H_{cc}^{(2)}]]^{-1}[H_{cc}^{(1)}]\}\{F_\beta^{(A)}\} \\ &\quad + \{[H_{cc}^{(1)}][[H_{cc}^{(1)}] + [H_{cc}^{(2)}]]^{-1}[H_{cr}^{(2)}]\}\{F_\gamma^{(A)}\}.\end{aligned} \tag{21}$$

A comparison of coefficients between equations (15) and (21) yields the following relationships:

$$\begin{aligned}[H_{\beta\alpha}](= [H_{\alpha\beta}]) &= [H_{cr}^{(1)}] - [H_{cc}^{(1)}][[H_{cc}^{(1)}] + [H_{cc}^{(2)}]]^{-1}[H_{cr}^{(1)}], \\ [H_{\beta\beta}] &= [H_{cc}^{(1)}] - [H_{cc}^{(1)}][[H_{cc}^{(1)}] + [H_{cc}^{(2)}]]^{-1}[H_{cc}^{(1)}], \\ [H_{\beta\gamma}](= [H_{\gamma\beta}]) &= [H_{cc}^{(1)}][[H_{cc}^{(1)}] + [H_{cc}^{(2)}]]^{-1}[H_{cr}^{(2)}].\end{aligned} \tag{22}$$

The same procedures can be applied to the first and last row in the assembled matrix, and then the following equations will be obtained

$$\begin{aligned}[H_{\alpha\alpha}] &= [H_{rr}^{(1)}] - [H_{rc}^{(1)}][[H_{cc}^{(1)}] + [H_{cc}^{(2)}]]^{-1}[H_{cr}^{(1)}], \\ [H_{\alpha\gamma}](= [H_{\gamma\alpha}]) &= [H_{rc}^{(1)}][[H_{cc}^{(1)}] + [H_{cc}^{(2)}]]^{-1}[H_{cr}^{(2)}], \\ [H_{\gamma\gamma}] &= [H_{rr}^{(2)}] - [H_{rc}^{(2)}][[H_{cc}^{(1)}] + [H_{cc}^{(2)}]]^{-1}[H_{cr}^{(2)}].\end{aligned} \tag{23}$$

The right-hand sides of equations (22) and (23) only contain the matrix of the substructure level. This means that $H_{ij}^{(A)}$ of the assembled structure can be calculated

directly from those of the rotor and the support structure. They can be expressed in a more compact form as follows:

$$\begin{bmatrix} [H_{\alpha\alpha}] & [H_{\alpha\beta}] & [H_{\alpha\gamma}] \\ [H_{\beta\alpha}] & [H_{\beta\beta}] & [H_{\beta\gamma}] \\ [H_{\gamma\alpha}] & [H_{\gamma\beta}] & [H_{\gamma\gamma}] \end{bmatrix} = \begin{bmatrix} [H_{rr}^{(1)}] & [H_{rc}^{(1)}] & [0] \\ [H_{cr}^{(1)}] & [H_{cc}^{(1)}] & [0] \\ [0] & [0] & [H_{rr}^{(2)}] \end{bmatrix}$$

$$- \begin{pmatrix} [H_{rc}^{(1)}] \\ [H_{cc}^{(1)}] \\ -[H_{rc}^{(2)}] \end{pmatrix} [[H_{cc}^{(1)}] + [H_{cc}^{(2)}]]^{-1} \begin{pmatrix} [H_{rc}^{(1)}] \\ [H_{cc}^{(1)}] \\ -[H_{rc}^{(2)}] \end{pmatrix}^{\mathrm{T}}. \tag{24}$$

3.2. IMPROVED ROTOR MODEL

3.2.1. *Equivalent models of the support structure*

Equivalent models can be regenerated, which have the same dynamic characteristics of the support structure. Support properties will be used for the coupled FRFs ($m = 1$) having both the driving and transfer functions in equation (12). Let us consider a serially connected spring–mass model with N degrees of freedom. Its mass and stiffness matrices can be written as

$$[M]_{eq} = \begin{bmatrix} m_1 & & & 0 \\ & m_2 & & \\ & & \ddots & \\ 0 & & & m_n \end{bmatrix}, \qquad [K]_{eq} = \begin{bmatrix} k_1 & -k_1 & & 0 \\ -k_1 & k_1 + k_2 & & \\ & & \ddots & \\ 0 & & & k_{n-1} + k_n \end{bmatrix}. \tag{25}$$

Thus, the dynamic behaviors of this system are described as follows:

$$\begin{pmatrix} X_1 \\ X_2 \\ \vdots \\ X_n \end{pmatrix} = \begin{bmatrix} H_{11} & H_{12} & & 0 \\ H_{21} & H_{22} & & \\ & & \ddots & \\ 0 & & & H_{nn} \end{bmatrix} \begin{pmatrix} F_1 \\ F_2 \\ \vdots \\ F_n \end{pmatrix}. \tag{26}$$

Equation (26) is an algebraic equation containing the system's frequency-dependent functions. We need, however, only consider a driving FRF $H_{11}(\omega)$, which corresponds to the receptance at any bearing position of the support structure. Its magnitude can be represented by the inversion of the dynamic stiffness matrix as

$$|H_{11}(\omega)| = \left| \frac{\beta_0 + \beta_1\omega^2 + \cdots + \beta_{n-1}\omega^{2n-2}}{\alpha_0 + \alpha_1\omega^2 + \cdots + \alpha_{n-1}\omega^{2n-2} + \alpha_n\omega^{2n}} \right|, \tag{27}$$

where

$$\beta_0 = k_2k_3 \cdots k_n + k_1k_3 \cdots k_n + \cdots + k_1k_2 \cdots k_{n-1},$$

$$\beta_1 = k_2k_3 \cdots k_{n-1}m_2 + k_2k_3 \cdots k_{n-2}k_nm_2 + \cdots + k_2k_3 \cdots k_{n-1}m_n,$$

TABLE 3

No. of coefficients of the regenerated model

DOF	β_0	β_1	β_2	β_3	β_4	β_5	β_6	α_0	α_1	α_2	α_3	α_4	α_5	α_6	α_7
2	2	1						1	31						
3	3	4	1					1	65	1					
4	4	10	6	1				1	10	15	5	1			
5	5	20	21	8	1			1	15	35	28	9	1		
6	6	35	56	36	101			1	21	70	84	45	11	1	
7	7	56	126	120	55	12	1	1	28	126	210	165	66	13	1

TABLE 4

Properties of the equivalent support model

	Support properties			
Model	Y direction		Z direction	
d.o.f.	$m_1 = 0{\cdot}036$	$k_1 = 6{\cdot}24\text{E}5$	$m_1 = 0{\cdot}125$	$k_1 = 1{\cdot}40\text{E}6$
	$m_2 = 0{\cdot}311$	$k_2 = 6{\cdot}23\text{E}5$	$m_2 = 1{\cdot}067$	$k_2 = 7{\cdot}21\text{E}6$
	$m_3 = 0{\cdot}793$	$k_3 = 2{\cdot}07\text{E}6$	$m_3 = 4{\cdot}834$	$k_3 = 1{\cdot}79\text{E}7$
Mass (kg), stiffness (N/mm)	$m_4 = 0{\cdot}868$	$k_4 = 1{\cdot}23\text{E}6$	$m_4 = 19{\cdot}06$	$k_4 = 7{\cdot}98\text{E}7$
	$m_5 = 3{\cdot}650$	$k_5 = 9{\cdot}64\text{E}6$	$m_5 = 205{\cdot}5$	$k_5 = 9{\cdot}90\text{E}8$
	$m_6 = 16{\cdot}76$	$k_6 = 4{\cdot}68\text{E}7$	$m_6 = 6264$	$k_6 = 15{\cdot}5\text{E}9$

$$\beta_{n-1} = m_2 m_3 \cdots m_n,$$

$$\alpha_0 = k_1 k_2 \cdots k_n,$$

$$\alpha_1 = k_1 k_2 \cdots k_{n-1} m_1 + k_1 k_2 \cdots k_{n-2} k_n m_1 + \cdots + k_1 k_2 \cdots k_{n-1} m_n,$$

$$\alpha_{n-1} = k_n m_1 m_2 \cdots m_{n-1} + k_{n-1} m_1 m_2 \cdots m_{n-1} + \cdots + k_1 m_2 m_3 \cdots m_n,$$

$$\alpha_n = m_1 m_2 m_3 \cdots m_n$$

and

$$\omega \to 0, \qquad H_{11}(0) = \frac{1}{k_1} + \frac{1}{k_2} + \cdots + \frac{1}{k_n}. \tag{28}$$

Therefore, we can extract the mass and stiffness elements by comparing the corresponding coefficients between equations (9) and (27). The regenerated dynamic properties provide an equivalent support model at any specified direction. These procedures can be applied for all connection co-ordinates between rotor and support.

However, note that the coefficients of equation (27) may be complicated according to the order of the interested model, the detailed information on the number of coefficients is listed in Table 3. It is proper to adapt a one higher degree-of-freedom (d.o.f.) model than the number of interested resonance of the structure and adequate numerically up to the 7-d.o.f. model. In this example, 6-d.o.f. models are used for both horizontal and vertical directions respectively, and the calculated results are listed in Table 4.

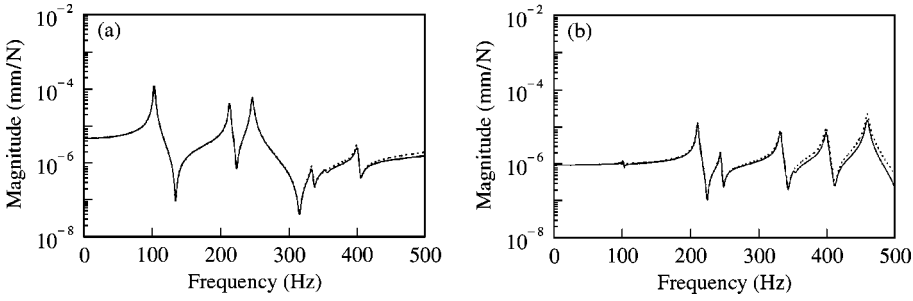

Figure 3. Comparison of the FRFs at the outboard bearing for the support structure and the regenerated equivalent model. (a) H_{YY}: ——, support FRF H_{YY}; ·····, regenerated FRF H_{YY} (without coupled effect). (b) H_{ZZ}: ——, support FRF H_{ZZ}; ·····, regenerated FRF H_{ZZ} (without coupled effect).

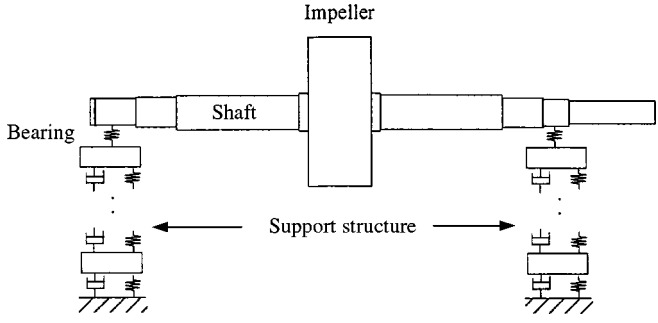

Figure 4. Improved rotor model.

Figure 3 shows the comparison of the FRFs between the support structure and the regenerated support model. It can be seen that the results are in good agreement.

3.2.2. *Improved rotor model*

The classical reduction techniques are generally interested in the identification of the modal parameters (natural frequencies, damping factors, and mode shapes) from the incomplete models. But, an improved rotor model is directly constructed by replacing the support structure as the equivalent models as shown in Figure 4. They are connected with the finite element rotor through the bearing positions. The baseplate of this problem is assumed to be rigid and the support structure to be rigidly restrained on the baseplate. The numerical analysis of this improved rotor will be performed by the finite element method. Therefore, the vibration behaviors of the assembled structure will be achieved efficiently although the support models have only a simple representation of the structure.

4. NUMERICAL RESULTS AND DISCUSSION

4.1. MODEL VALIDATION

To illustrate the efficiency and accuracy of the present methods, frequency response analyses are performed at rest by using MSC/NASTRAN. Under a unit load harmonic

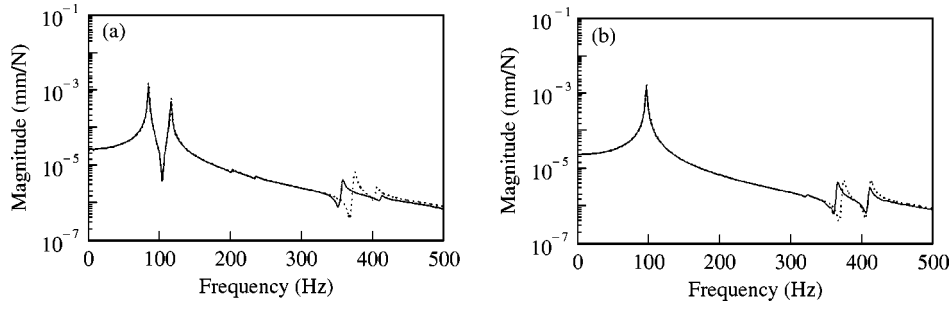

Figure 5. Comparison of the receptance at impeller center between the pump system and the impedance coupling method. (a) $H_{YY}(\omega)$: ——, full system FRF H_{YY}; · · · · ·, impedance coupled method FRF H_{YY}. (b) $H_{ZZ}(\omega)$: ——, full system FRF H_{ZZ}; · · · · ·, impedance coupled method FRF H_{ZZ}.

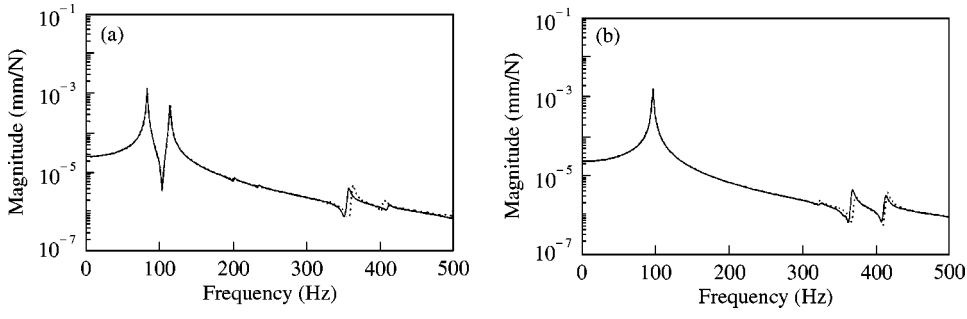

Figure 6. Comparison of the receptance at impeller center between the pump system and the improved rotor model. (a) $H_{YY}(\omega)$: ——, full system FRF H_{YY}; · · · · ·, equivalent shaft FRF H_{YY}. (b) $H_{ZZ}(\omega)$: ——, full system FRF H_{ZZ}; · · · · ·, equivalent shaft method FRF H_{ZZ}.

excitation at the impeller center, the vibration responses are obtained at the same location and compared to those of the system model.

Figure 5 shows the receptance magnitudes in horizontal and vertical directions respectively. The results of the impedance coupling method agree well with those of the pump system. The correspondent vibration magnitudes of the improved rotor together with those of the system model are also depicted in Figure 6. They show that the response of the vertical direction is not nearly affected by the support dynamics over a range from 0 to 300 Hz.

This fact can also be inferred from the FRFs of the support structure. The first resonance of the vertical direction is far from that of the rotor model (99·2 Hz). So, it may be concluded that the resonances of the rotor are reduced and additional natural frequencies may be introduced due to the support dynamics, and the support effects are more significant as the resonances of the support structure are closer to those of the rotor model.

4.2. VIBRATION ANALYSIS OF THE ROTOR

The proposed techniques are applied for calculating the natural frequencies and the unbalance responses of the rotor. The natural frequencies of the rotor system are commonly called the critical speeds, at which vibration amplitude due to unbalance is a local maximum, and they may be changed as the variation of the rotating speed.

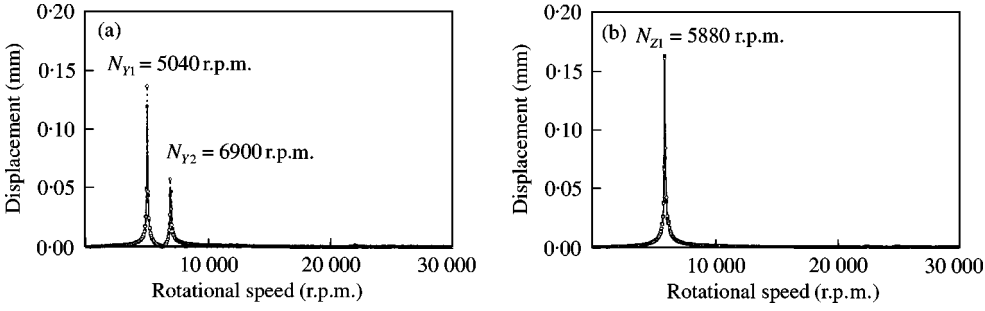

Figure 7. Unbalance responses at impeller center for the impedance coupling method and the improved rotor model. (a) Horizontal; (b) vertical directions: —•—, Equivalently supported rotor; ···•···, impedance coupled method.

Figure 7 shows the synchronous whirl amplitudes by the presented techniques. Because of the dynamic asymmetry of the support structure, the amplitudes of both directions are unequal and the additional critical speeds are introduced in the horizontal direction. But, they show good agreement with each other.

5. CONCLUSIONS

For more reliable results of rotordynamic analyses, the support effects need to be necessarily considered in the rotor-bearing system. In this study, the improved rotor model including the support effects is suggested. Its results agree well with the other analysis method (impedance coupling method). So, the proposed method is regarded as a useful tool for the vibration analysis of the rotor operating on the flexible structure. However, as indicated previously, the advantage of the method is diminished by increasing the number of d.o.f. in the regenerated support model, because the computation time required to find the polynomial coefficients increases.

REFERENCES

1. B. S. YANG, S. K. OH and T. IWATSUBO 1986 *Transactions of the KSME* **10**, 56–61. Effects of annular seals on the stability of centrifugal pump rotors.
2. T. N. SHIAU and J. L. HWANG 1989 *Journal of Vibration, Acoustics, Stress and Reliability in Design* **111**, 379–385. A new approach to the dynamic characteristic of undamped rotor-bearing systems.
3. G. SAUER and M. WOLF 1989 *Finite Elements in Analysis and Design* **5**, 131–140. Finite element analysis of gyroscopic effects.
4. D. KIM and J. W. DAVID 1990 *Transactions of the American Society of Mechanical Engineers, Journal of Vibration and Acoustics* **112**, 112–118. An improved method for stability and damped critical speeds of rotor-bearing systems.
5. B. T. MURPHY 1993 *American Society of Mechanical Engineers, Vibration of Rotating Systems* **60**, 35–42. Improved rotor dynamic unbalance response calculations using the polynomial method.
6. L. FORRAI 1996 *American Society of Mechanical Engineers*, **96-GT-407** NY, 1–4. Stability analysis of symmetrical rotor-bearing systems with internal damping using finite element analysis.
7. J. M. VANCE 1987 *Rotordynamics of Turbomachinery*. New York: John Wiley & Sons., Inc.
8. C. W. LEE 1993 *Vibration Analysis of Rotors*. Dordrecht: Kluwer Academic Publishers.
9. L. M. GREENHILL and G. A. CORNEJO 1995 *Design Engineering Technical Conference* DE **84**, 991–1000. Critical speed analysis resulting unbalance excitation of backward whirl modes.

10. J. R. BUCKLES, K. E. ROUCH and J. R. BAKER 1996 *American Society of Mechanical Engineers*, **96-GT-403** NY, 1–9. Modelling support effects—finite element and experimental modal methods.
11. A. OKITSU, K. YAMASHITA and H. AZEGAMI 1987 *JSME* **54**, 2059–2064. Substructure synthesis method with consideration of rotational effects on the combined boundary.
12. S. W. HONG and J. H. PARK 1996 *Journal of KSNVE* **6**, 71–82. On improved substructure synthesis method for unbalance response analysis of rotor bearing systems.
13. H. TAIPING 1988 *Transactions of American Society of Mechanical Engineers, Journal of Vibration, Acoustics, Stress, and Reliability in Design* **110**, 468–472. The transfer matrix impedance coupling method for the eigensolutions of multi-spool rotor systems.
14. B. YANG 1992 *Journal of Sound and Vibration* **159**, 23–37. Natural frequencies of combined gyroscopic systems.
15. L. E. SUAREZ and M. P. SINGH 1992 *Journal of Engineering Mechanics* **118-7**, 1488–1503. Modal synthesis method for general dynamic systems.
16. D. E. EWINS 1986 *Modal Testing: Theory and Practice*. Letchwor: Research Studies Press Ltd.
17. L. W. CHEN and D. M. KU 1992 *Transactions of the American Society of Mechanical Engineers, Journal of Vibration and Acoustics* **114**, 326–329. Dynamic stability of a cantilever shaft-disk system.
18. T. Y. CHEN and B. P. WANG 1993 *Transactions of the American Society of Mechanical Engineers, Journal of Engineering for Gas Turbines and Power* **115**, 256–260. Optimum design of rotor-bearing systems with eigenvalue constraints.
19. A. HOUMAT 1995 *Journal of Sound and Vibration* **187**, 841–849. Vibrations of Timoshenko beams by variable order finite elements.
20. Q. H. QIN and C. X. MAO 1996 *Computers and Structures* **58**, 835–843, Coupled tortional-flexural vibration of shaft systems in mechanical engineering—I. Finite element model.
21. J. S. RAO 1991 *Rotor Dynamics*. New York: John Wiley & Sons.
22. T. A. HARRIS 1966 *Rolling Bearing Analysis*. New York: John Wiley & Sons.
23. B. JETMUNDSEN, R. L. BIELAWA and W. G. FLANNELLY 1988 *Journal of the American Helicopter Society*, 55–64. Generalized frequency domain substructure synthesis.
24. Y. REN 1993 *Internal Modal Analysis Conference*, 868–871. A Generalized Receptance Coupling Technique.
25. E. KRAMER 1993 *Dynamics of Rotors and Foundation*. Berlin: Springer-Verlag.